Dynamics of electric-field-induced molecular reorientation and segmental mobility in the smectic-C^* phase of a ferroelectric liquid crystal: Faster reorientation of cores than the alkyl chains revealed by time-resolved infrared spectroscopy

A. L. Verma,[1,2,*] B. Zhao,[1,3] S. M. Jiang,[3] J. C. Sheng,[3] and Y. Ozaki[1,*]

[1]*School of Science, Kwansei-Gakuin University, Uegahara, Nishinomiya 662, Japan*
[2]*Department of Physics, North-Eastern Hill University, Shillong-793022, India*
[3]*Key Laboratory of Supramolecular Structure and Spectroscopy, Jilin University,*
Changchun, 130023, People's Republic of China

We report a study of the dynamics of molecular reorientation and segmental mobility of a ferroelectric liquid crystal in the smectic-C^* (Sm-C^*) phase having 2-hydroxy-benzilidenianiline as the mesogen core and (S)-2-chloro-3-methylbutanoyl as the chiral terminal group, at different temperatures during electric-field-induced switching between the two surface-stabilized states by use of a time-resolved Fourier-transform infrared technique. From polarized infrared spectra under static dc electric fields, details of mutual arrangement of different molecular segments in the Sm-C^* phase have been obtained. Contrary to the usual expectations, the average alkyl chain axis does not coincide with the mesogen axis and is less tilted with respect to the layer normal than the mesogen. On the other hand, motion of the carbonyl groups is found to be strongly hindered and the distribution function for the C=O bonds is not cylindrically symmetric with respect to the long molecular axis. Time-resolved infrared measurements at different temperatures and voltages have revealed that, on switching the polarity of the electric field, the hydrogen-bonded C=O group moves with the mesogen which reaches equilibrium orientations at a faster rate compared to the alkyl chain at the temperatures and voltages employed in this study. [S1063-651X(97)09209-X]

PACS number(s): 61.30.−v, 78.47.+p

I. INTRODUCTION

The surface-stabilized ferroelectric liquid crystals (SS-FLC) in the smectic-C^* (Sm-C^*) phase are some of the most interesting liquid crystals (LC) because of their potential applications in high resolution flat panel displays and fast electro-optic devices [1–6]. The physical and electro-optical properties of ferroelectric liquid crystals (FLC) are strongly dependent on their molecular shape and local environment which determine the statistical distribution and equilibrium population of each conformational state of the molecules. When a FLC in the Sm-C^* phase is placed inside a cell of a few μm thickness, the average long molecular axis aligns along two directions at temperature-dependent angles from the normal to the smectic layers which are called the surface-stabilized states [1,5]. By reversing the polarity of the applied electric field, molecules can be switched back and forth from one state to the other state at a fast speed in the microsecond range. The electric field interacts with the polarization and dielectric anisotropy of the molecules in the process of electro-optical switching, which depends strongly on the molecular conformation and orientational freedom of different segments about the average long molecular axis. Specifically, the alkyl chain orientation with respect to the rigid core and hindered rotation of molecular segments like carbonyl groups having large dipole moment located near the chiral carbon are expected to play an important role in the emergence of spontaneous polarization and thus may influence

the dynamical behavior of the system.

Despite the great promise of FLC's having fast response and excellent electro-optical properties, the detailed mechanism of field-induced reorientation of different segments of FLC's is not yet fully elucidated due to the complexity of their structure, and the nonavailability of suitable time-resolved experimental techniques to probe structural details at the molecular level. As the vibrational frequencies are very sensitive to small changes in the bonding and geometrical arrangement of atoms in molecules, infrared absorption and Raman scattering techniques can provide very useful information about the conformation and hindered rotational motions of individual segments of LC molecules. During the recent past, time-resolved Fourier-transform infrared (FT-IR) spectroscopy has been developed and applied as a powerful tool for investigating the dynamics of electric-field-induced switching of FLC's [7–27]. Contrary to the commonly accepted belief that the mesogen (rigid core) and the flexible alkyl chain reorient as rigid units in LC's [7–13,15–17], it has recently been observed [24] that in a chiral smectic-A liquid crystal, the molecular tails are less tilted than the cores with respect to the smectic layer normal and the reorientation rate of the mesogen is faster than that of the alkyl chain during switching. On the other hand, polarized FT-IR studies on a series of antiferroelectric LC's [25–27] revealed that all the molecular segments reorient simultaneously at the same rate while the carbonyl groups in both the chiral and core parts are hindered, though the polarization dependence of the absorbance peaks of the C=O groups in the Sm-C^* phase did not show much change [25]. The other recent studies on nematic LC's and liquid crystalline polymers [22,23] have

---

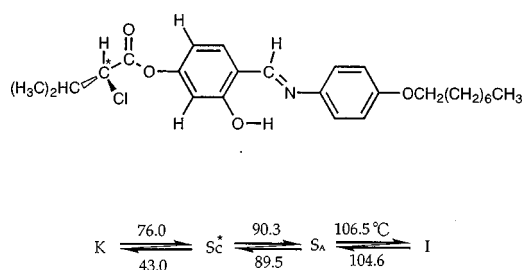*Authors to whom correspondence should be addressed.

FIG. 1. Structure of the VOH8 ferroelectric liquid crystal and phase transition temperature.

also explored the orientational dynamics and mobility of different segments under applied electric fields. However, the understanding of reorientational behavior in chiral Sm-C^* phases of FLC's is far from clear.

In this work we report time-resolved FT-IR studies of electric-field-induced reorientation and segmental mobility in a chiral ferroelectric liquid crystal having 2-hydroxy-benzilidenianiline as the mesogen core and (S)-2-chloro-3-methylbutanoyl as the chiral terminal group, named VOH8, in the Sm-C^* phase at different temperatures and voltages. Our studies have provided unambiguous evidence that the average alkyl chain and mesogen axes do not coincide in the equilibrium state, the motion of the carbonyl group is strongly hindered, and its orientation is biased in one direction with respect to the long molecular axis. The time-resolved measurements clearly show that the messages reorient at a faster rate while the alkyl chains lag behind the mesogen during switching at all the temperatures and applied voltages used in this study.

II. EXPERIMENT

The chemical structure along with the phase transition temperatures of the investigated chiral ferroelectric liquid crystal, VOH8, are shown in Fig. 1. The synthesis of this liquid crystal has been reported in Ref. [28]. The introduction of an OH group at the *ortho* position of the aromatic ring increases its stability due to intramolecular hydrogen bonding and the system exhibits a wider temperature range than the compound without the OH group in the Sm-C^* phase on cooling from the smectic-A phase. The sample cell consisted of two BaF_2 plates coated with conducting layers of indium tin oxide (ITO) and polyvinyl alcohol rubbed in one direction. The thickness between the two plates, as determined from the interference fringe pattern, was adjusted to 3.7 μm with a polyethylene spacer. The cell was filled from the melted sample by capillary action, heated to the isotropic phase, and then slowly cooled down to a temperature in the Sm-C^* phase. temperature was controlled to an accuracy of ±0.05 °C with the aid of an Omron E5T thermocontroller and Peltier element.

The polarized IR spectra on a well aligned monodomain of the sample were measured on a JEOL Model JIR-6500 FT-IR spectrometer equipped with a JEOL Model IR-MAU 100 microattachment and a meercury-cadmium-tellurium (MCT) detector. The approximate size of the monodomain was in a several hundred μm range. A wire grid polarizer was rotated about the axis parallel to the propagation direction of the radiation. The measurement geometries are sche-
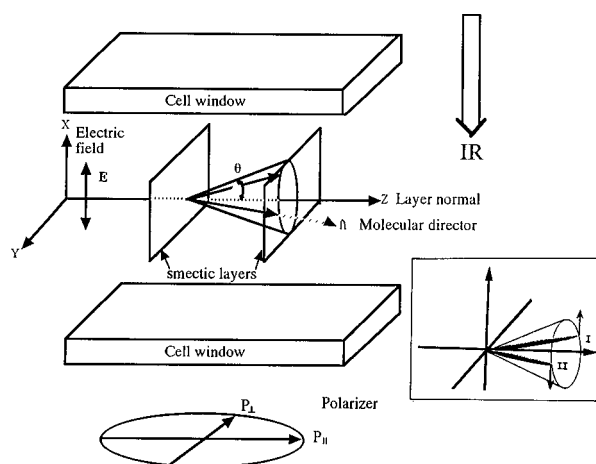

FIG. 2. Schematic arrangement for the time-resolved infrared measurements. I and II are the projections of the directions of the molecular long axis in the plane of the cell window, YZ (surface-stabilized states of the FLC), θ is the angle between the projection of the molecular long axis and the projection of the smectic layer normal in the plane of the cell windows (broken line parallel to the rubbing direction, Z), E is the direction of the applied electric field, X is the direction of the infrared light, $P_{\parallel}$ and $P_{\perp}$ represent the horizontal and vertical polarizations of the light, respectively. Inset: the designations I and II.

matically shown in Fig. 2, where the horizontal broken line indicates the projection of the smectic layer normal in the plane of the cell windows, which is considered parallel to the rubbing direction. The two surface-stabilized states are indicated by arrows I and II, which are the projections of the long molecular axes in the plane of the cell windows in states I and II. The polarized IR spectra were measured under dc applied voltages of 0, 5, and 7 V of both polarities at 83 °C and 75 °C. The polarization angle is taken as zero when the polarization direction of the incident IR radiation coincides with the broken line in the rubbing direction.

Time-resolved measurements were made by use of the same FT-IR spectrometer working in the asynchronous mode equipped with a boxcar integrator (Stanford Research System SR 250) consisting of a gate circuit and a pulse delay circuit. A rectangular electric field of ±3, ±5, and ±7 V and 5 KHz repetition rate was applied between the electrodes of the cell from a function generator (Kenwood FG-273). The gate of the boxcar integrator was opened for 5 μs after $5n$ ($n=0,1,2,...$) μs from the rise of the voltage pulse. Thus time-resolved spectra were measured from 0 to 100 μs at intervals of 5 μs at a resolution of 4 cm^{-1} by averaging 200 spectra. As the largest intensity changes were observed when the polarizer direction was at 45° to the rubbing direction, most of the time-resolved spectra were measured with this fixed position of the polarizer at 45°. We also measured the polarization-dependent spectra from 0° to 180° at delay times of 0, 20, and 100 μs to investigate further details of the switching mechanism.

The spectra were corrected for a baseline using a nonlinear spline function, and bands arising from the water vapors in the spectrometer were subtracted. In order to separate the overlapping bands, the IR spectra were curve fitted using the GRAMS program, and the areas and heights of the separated bands were used for further processing of the data.
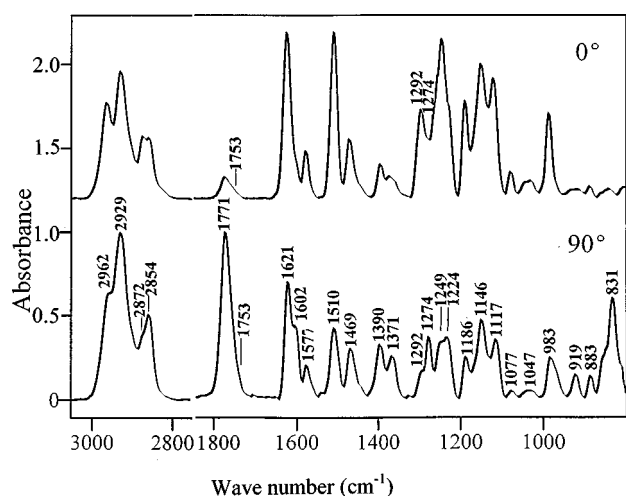
FIG. 3. Polarized FT-IR spectra of VOH8 at 83 °C in the (a) parallel ($\omega = 0°$) and (b) perpendicular ($\omega = 0°$) polarization geometries. Resolution, 4 cm^{-1}; accumulation, 500 times.

III. RESULTS AND DISCUSSION

A. Mutual arrangement of molecular segments in equilibrium

We shall first discuss the static FT-IR results for the FLC in the Sm-C^* phase to derive information about the mutual arrangement of different molecular segments in their average equilibrium state. Figure 3 shows the polarized IR spectra as a function of polarization angle ω for a monodomain of the sample in the Sm-C^* phase at $\omega = 0°$ and 90°. The polarization angle ω is defined as the angle between the rubbing direction (smectic layer normal) and the polarization direction of the incident IR radiation and is taken as zero when these two directions coincide. From these spectra, the dichroic ratio D, defined as the ratio of the absorbances for the parallel and perpendicular polarizations of light, for the absorption bands was calculated. The most probable assignment [29] and dichroic ratios for the isolated and relevant bands are listed in Table I. The high value of the dichroic ratios for some of the bands associated with the mesogen moiety shows that the degree of orientational order in the Sm-C^* phase is really high. However, one may notice from Table I that the dichroic ratio for the C—O stretching mode at 1292 cm^{-1} is 5.7, while it varies from 4.8 to 2.5 for the benzene rings C=C, and the C=N stretching modes, indicating that the two benzene rings may be slightly skewed with respect to each other [30]. The vibrational bands associated with the alkyl chain modes exhibit dichroic ratios of ≤ 1 due to disorder in the chain, which is supported by higher wave numbers of the CH$_2$ symmetric (2854 cm^{-1}) and antisymmetric (2929 cm^{-1}) stretching modes, characteristics of substantial gauche conformations in the hydrocarbon chain [31]. The C=O stretching mode splits into two components at 1771 and 1753 cm^{-1} where the latter component may arise from either the hydrogen-bonded C=O group with the phenyl ring proton, or may originate from another rotational conformation of the molecule. As the variation of intensities of the two components shows different behavior during dynamical switching, and based on the estimated orientations of the transition dipoles and dichroic ratios, we believe that the second component at 1753 cm^{-1} originates from hydrogen bonding. We shall denote the 1771 1753 cm^{-1} components as arising from the C=O (free), and C=O (H-bonded) groups, respectively.

TABLE I. Dichroic ratio (D) and vibrational band assignment for the relevant peaks in the infrared spectra of VOH8 liquid crystal in the Sm-C^* phase.

Wave number (cm^{-1})[a]	$D(A_\parallel / A_\perp)$	Assignment[b]
2962(m)	1.0	CH$_3$ asym. st.
2929(s)	0.5	CH$_2$ antisym. st.
2901(sh)	1.0	CH st.
2872(m)	1.0	CH$_3$ sym. st.
2854(m)	0.8	CH$_2$ sym. st.
1771(m)	0.2	C=O st. (free)
1753(w)	0.4	C=O st. (hydrogen bonded)
1621(s)	3.0	C=N st.
1577(m)	2.5	phenyl ring C=C st.
1510(s)	4.8	phenyl ring C=C st.
1469(m)		CH$_2$ def.
1292(m)	5.7	C—O st.
1274(m)	1.2	C—OH st.
1249(m,sh)	5.4	C—O st.
1186(m)	4.0	phenyl ring C—C def.
1146(m)	3.0	chain C—C st.
1117(m)	3.2	phenyl ring C—C def.
1077(w,sh)	4.5	phenyl ring C—C def.
983(m)	4.3	phenyl ring C—H in-plane def.
883(w)	0.4	phenyl ring C—H out-of-plane def.
831(w)	0.2	phenyl ring C—H out-of-plane def.

[a]w, weak; m, medium; s, strong; sh, shoulder.

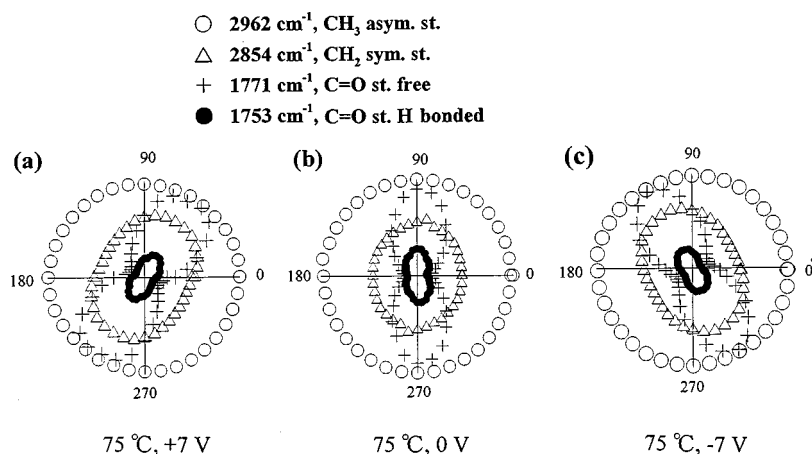[b]sym, symmetric; asym, asymmetric, antisymmetric; st, stretching; def, deformation.

○ 2962 cm⁻¹, CH₃ asym. st.
△ 2854 cm⁻¹, CH₂ sym. st.
+ 1771 cm⁻¹, C=O st. free
● 1753 cm⁻¹, C=O st. H bonded

(a) **(b)** **(c)**

75 ℃, +7 V   75 ℃, 0 V   75 ℃, -7 V

FIG. 4. Polar plots of the peak absorbance $A(\omega)$ vs the polarization angle ω for the representative bands from the alkyl chain and the C=O groups of the VOH8 in the Sm-C^* monodomain at 75 °C under dc electric fields of (a) +7 V, (b) 0 V, and (c) −7 V across the cell of thickness 3.7 μm.

In order to characterize and monitor the behavior of different molecular moieties, we have chosen the comparatively isolated bands at 2854 (CH₂ symmetric stretching) and 2962 (CH₃ asymmetric stretching) cm⁻¹ for the alkyl chain, 1771 ($\nu_{C=O\text{ free}}$), and 1753 ($\nu_{C=OH\text{-bonded}}$) cm⁻¹ bands for the chiral part, and the 1510 ($\nu_{C=C}$), 1621 ($\nu_{C=N}$), and 983 (phenyl ring C—H in-plane deformation) cm⁻¹ bands for the mesogen part. In our system, the CH₂ groups are located in only the alkyl chain part and therefore it is possible to monitor the alkyl chain movement distinctly without overlapping of the bands from the chiral or mesogen parts. At zero applied voltage, the mesogen bands show parallel dichroism with intensity maxima at $\omega = 0°$ or 180° while the C=O and alkyl chain modes exhibit perpendicular dichroism with I_{max} at $\omega = 90°$ or 270°.

Polarization-dependent IR spectra of the sample in the Sm-C^* phase were measured at 83 °C and 75 °C under dc voltages of 0, 7, and 5 V with positive and negative polarity for monitoring the relative orientation of the alkyl chain, mesogen, and the chiral segments. The polarization dependence of absorption peaks is conveniently described by polar plots where the peak absorbance $A(\omega)$ at a particular polarization angle ω is plotted as a function of ω. Figures 4 and 5 show the polar plots of $A(\omega)$ vs ω for the representative peaks of the alkyl chain and the C=O groups; and for the mesogen bands, respectively, at 75 °C on application of dc electric fields of +7 (a), 0 (b), and −7 (c) V. It is clear from these figures that the absorbances of the bands from the three segments attain their maxima at different angles of polariza-

tion while the absorbance due to the CH₃ stretching mode at 2962 cm⁻¹ scarcely depends on ω. Most interesting of all of these is the behavior of the peaks associated with the C=O groups which show maxima at different polarization angles for the positive and negative polarity of the electric field. For example, at 75 °C and +7 V, the $A(\omega)$ maximizes at 30° while it shows maximum at 35° at −7 V. The estimated uncertainty in the measurement of the polarization angles was ±1°, so that the difference between 30° and 35° is significant. A similar effect was observed at 83 °C for electric fields of 7 and 5 V of opposite polarity. As the transition moments of the 1510, 1621, and 983 cm⁻¹ bands are nearly parallel to the long mesogen axis, the observed rotation of the absorption maxima of these bands between the positive and negative polarity of the electric fields by an angle of $\Delta\omega = 58°$ at 75 °C and 7 V, 60° at 83 °C and 7 V, and 53° at 83 °C and 5 V corresponds to the rotation of the mesogen by the same angles. On the other hand, the absorption maximum of the CH₂ symmetric stretching band rotates by $\Delta\omega = 48°$ at 75 °C and 7 V, 54° at 83 °C and 7 V, and 44° at 83 °C at 5 V, respectively. These results are very significant and provide unambiguous evidence for hindered rotation of the chiral group, and nonlinearity of the alkyl and chiral chains with the mesogen and molecular long axis. When the polarity of the applied field is reversed, the alkyl chain rotates to a lesser extent than the mesogen, implying that the average alkyl chain axis does not coincide with the average direction of the long molecular axis. The peculiar behavior of the C=O
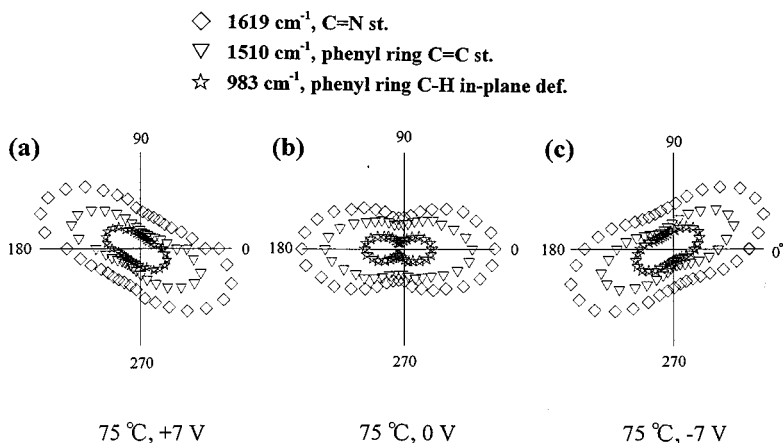
◇ 1619 cm⁻¹, C=N st.
▽ 1510 cm⁻¹, phenyl ring C=C st.
☆ 983 cm⁻¹, phenyl ring C-H in-plane def.

(a) **(b)** **(c)**

75 ℃, +7 V   75 ℃, 0 V   75 ℃, -7 V

FIG. 5. Polar plots of the peak absorbance $A(\omega)$ vs the polarization angle ω for the three representative bands of the mesogen segment of the VOH8 in the Sm-C^* monodomain at 75 °C under dc electric fields of (a) +7 V, (b) 0 V, and (c) −7 V across the cell of thickness 3.7 μm.
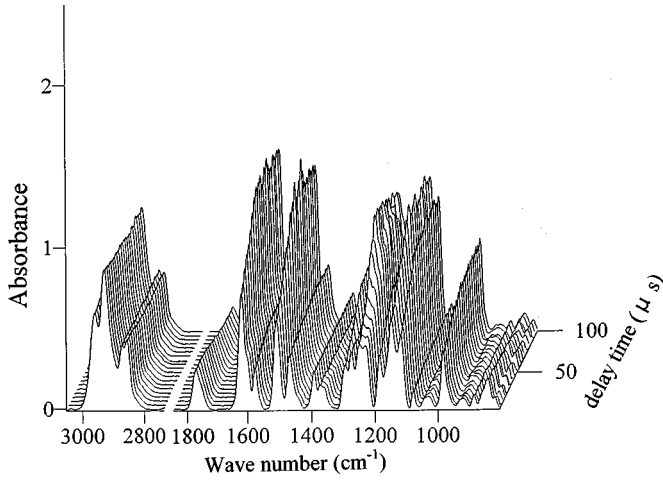
FIG. 6. Time-resolved FT-IR spectra of VOH8 in the Sm-C^* phase at 83 °C under an electric field of ± 5 V and 5 kHz repetition rate as a function of delay time from 0 to 100 μs at intervals of 5 μs.

bands clearly indicates hindered rotation of the C=O groups and the nonsymmetrical distribution function of the C=O bonds around the long mesogen axis.

For a ferroelectric liquid crystal in which the Sm-C^* phase is obtained from the Sm-A phase through a second order phase transition, the optical tilt angle $\theta(T)$ varies with temperature as

$$\theta(T) = \theta_0 (T_c - T)^\beta,$$

where θ_0 is a temperature-independent constant tilt angle, T_c (°C) is the Curie temperature for the Sm-A–Sm-C^* transition, and the average value of the exponent β is ~ 0.5 in a limited temperature range [6]. Moreover, the induced tilt angle increases linearly with the applied electric field. When $(T_c - T)$ is ~ 10 °C, the tilt angle $\theta(T)$ becomes nearly constant. The rotation of the mesogen segment at different temperatures and electric fields is in conformity with these relations, which are valid in the approximation of the whole molecule orienting as a single entity. The orientational motion of the alkyl chain and the C=O groups appears to be a more complicated process than can be understood from these relations.

If we consider a vibrational mode N which has a transition dipole moment μ_N oriented at a fixed angle α_N with respect to the molecular long axis $\mathbf{M}$, which in turn, is oriented at an angle θ to the mean orientation $\mathbf{n}$, then the long axis order parameter about $\mathbf{n}$ is given by [32]
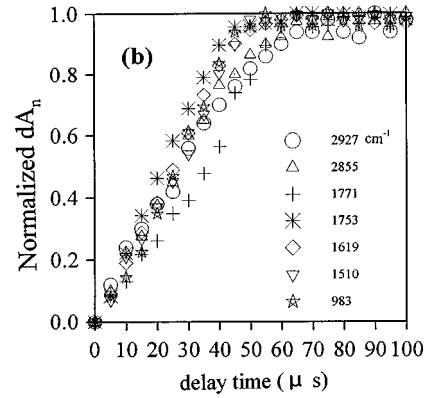
$$S = \langle P_2(\cos\theta) \rangle = \tfrac{1}{2} \langle (3\cos^2\theta - 1) \rangle,$$

where $P_2(\cos\theta)$ is the Legendre polynomial of order 2, and the angle bracket indicates average value. The dichroic ratio for an absorption band with its transition dipole moment oriented at an angle α_N relative to the molecular long axis is defined as
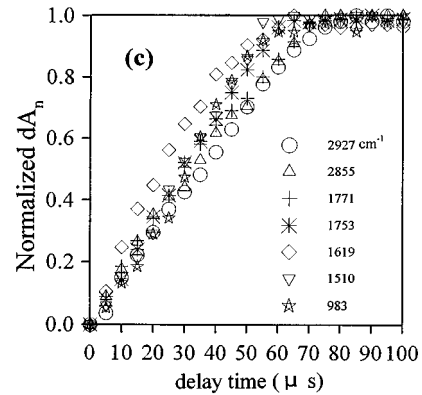
$$D(S, \alpha_N) = A(0)/A(90)$$

$$= [1 + 2P_2(\cos\alpha_N)S]/[1 - 2P_2(\cos\alpha_N)S]$$
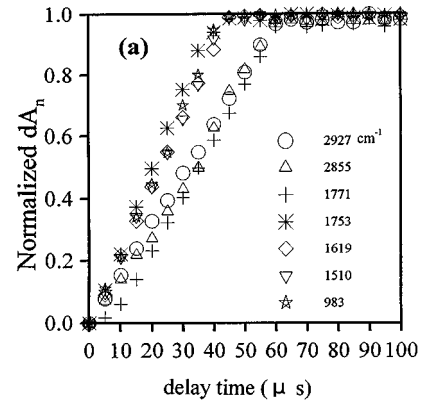
83 °C, ± 7 V, 5kHz

83 °C, ± 5 V, 5kHz

83 °C, ± 3 V, 5kHz

FIG. 7. Time dependence of normalized intensity changes (dA_n) vs delay time for representative infrared bands characteristic of the mesogen, alkyl chain, and the chiral segments of VOH8 in the Sm-C^* phase at 83 °C under an electric field of 5 kHz repetition rate at (a) ± 7 V, (b) ± 5 V, and (c) ± 3 V.

from which the mean orientation of the transition dipole moment with respect to the average long molecular axis is obtained as

$$\cos^2\alpha_N = 1/3[2(D-1)/S(D+2) + 1].$$

Since large values of $D = 5.7$ and 5.4 were observed for the C—O stretching modes at 1292 and 1249 cm^{-1} from

TABLE II. Electric field strength, and temperature dependence of the reorientation times (in μs) of different segments for the VOH8 liquid crystal in the Sm-C^* phase.

Segment	Temperature 83 °C Applied voltage			Temperature 75 °C Applied voltage	
	± 3 V	± 5 V	± 7 V	± 5 V	± 7 V
$\nu C\!\!=\!\!O$ free and alkyl chain	75 μs	65 μs	62 μs	70 μs	64 μs
$\nu_{C\!=\!O}$ H bonded and mesogen	65 μs	50 μs	45 μs	59 μs	53 μs

the terminal carbonyl groups, we can assume that the transition dipole moment for these bands lies along the long molecular axis (i.e., $\theta_{1292}=0$). For $D=5.7$ we obtain a value of 0.61 for long axis order parameter S. From the measured dichroic ratio of the bands, we calculate the mean orientation of transition dipole moments and obtain average values of α as 51°, 75°, 90°, 28°, and 14°, for the $\nu_{C\!-\!OH}$ at 1274 cm^{-1}, $\nu_{C\!=\!O}$ (H bonded) at 1753 cm^{-1}, $\nu_{C\!=\!O}$ (free) at 1771 cm^{-1}, $\nu_{C\!=\!N}$ at 1621 cm^{-1}, and $\nu_{C\!=\!C}$ (phenyl) at 1510 cm^{-1} modes, respectively. The C—OH group attached to the phenyl ring is H bonded with the C=N and is expected to have its transition dipole moment oriented nominally at $\alpha_{C\!-\!OH} \sim 60°$. The calculated α values for other bands also deviate from such expectations, indicating that the deviations from isotropic averaging for different functional groups about the long molecular axis are not negligible.

The orientational behavior of the C=O groups is particularly interesting. If the C=O groups rotated freely along the long molecular axis, the angular dependence of the C=O peaks should be symmetrical with respect to the phenyl (or C—O) peaks. On the other hand, if the motion of the C=O groups is hindered and if they oriented along the applied electric field perpendicular to the cell windows, no absorption would be expected from the C=O stretching modes. The experimental results indicate that the orientation of the C=O groups is biased in a specific direction with respect to the average long molecular axis direction with an asymmetrical position. Furthermore, the most probable orientation of the C=O groups is not in the plane containing the C_2 axis of the Sm-C^* phase. In other words, the orientational distribution of the C=O groups is not mirror symmetric with the tilting plane and the spatial position of the transition moment of the C=O band is not symmetrical with respect to the average long molecular axis.

Based on these results, we propose the following static model for segmental arrangement in equilibrium in the Sm-C^* phase of the VOH8 liquid crystal. The mesogen and the alkyl chain are tilted at different angles with respect to the smectic layer normal and the magnitudes of the tilts depend upon the temperature and applied voltage. The alkyl chains are not in the all-*trans* conformation but have substantial disorder as indicated by the presence of gauche conformations. The rotation of the carbonyl groups is strongly hindered, and its orientation is biased in a unique direction in an unsymmetrical position to the tilting plane. Reversing the polarity of the applied field rotates the C=O groups to a new position which is not identical with the former position for rotation of 180° around the layer normal, **n**.

B. Segmental mobility and dynamical behavior during switching

In order to explore the possibilities of detecting conformational changes from the orientational changes during switching from one to another surface-stabilized state on change of polarity of the electric field, time-resolved FT-IR spectra with 5 μs resolution were measured at 83 °C and 75 °C at applied voltages of ± 3, ± 5, and ± 7 V of 5 kHz repetition rate. Figure 6 shows the time-resolved spectra at 83 °C and ± 5 V as a function of delay time from 0 to 100 μs. Each spectrum represents the absorbance change from the spectrum at zero delay time taken as a reference. From these figures one can see that almost all the bands change their intensity when polarity of the field is reversed, meaning that all segments of the molecule participate in the reorientation process. As the tilt angle varies with the applied electric field and temperature, we calculated the normalized absorbance changes dA_n for a quantitative comparison of the reorientation rates of molecular segments at different temperatures and voltages as follows:

$$dA_n = [A(t)-A(2)]/[A(1)-A(2)],$$

where $A(t)$ is the peak absorbance at time t, and $A(1)$ and $A(2)$ are the peak absorbance values at the stabilized states I (before the application of electric field) and II (when the reorientation is completed), respectively. These plots also give information about fractional reorientation of the segments of the molecule at a particular time. Figures 7(b), and 7(c) give the plot of dA_n vs delay time during the course of switching for selected bands characterizing the mesogen, chiral, and alkyl chain segments at 83 °C at ± 3, ± 5, and ± 7 V amplitudes of the voltage pulse.

These figures make it clear that the reorientation from one state towards another state starts immediately on change of polarity of the applied field and after a certain time, the molecule attains the second surface-stabilized position. However, the different segments reorient at distinct and different times. Similar behavior was observed at 75 °C at applied voltages of ± 5 and ± 7 V. Table II summarizes the results of the effect of electric field strength and temperature on the average time for completion of reorientation of different segments.

For understanding these variations of reorientation times, we recall that the temperature dependence of the intrinsic electro-optic response time τ for a SSFLC is proportional to $[\gamma_\varphi(T)]/[P(T)E]$ where $\gamma_\varphi(T)$ and $P(T)$ are the temperature-dependent reorientational viscosity and sponta-
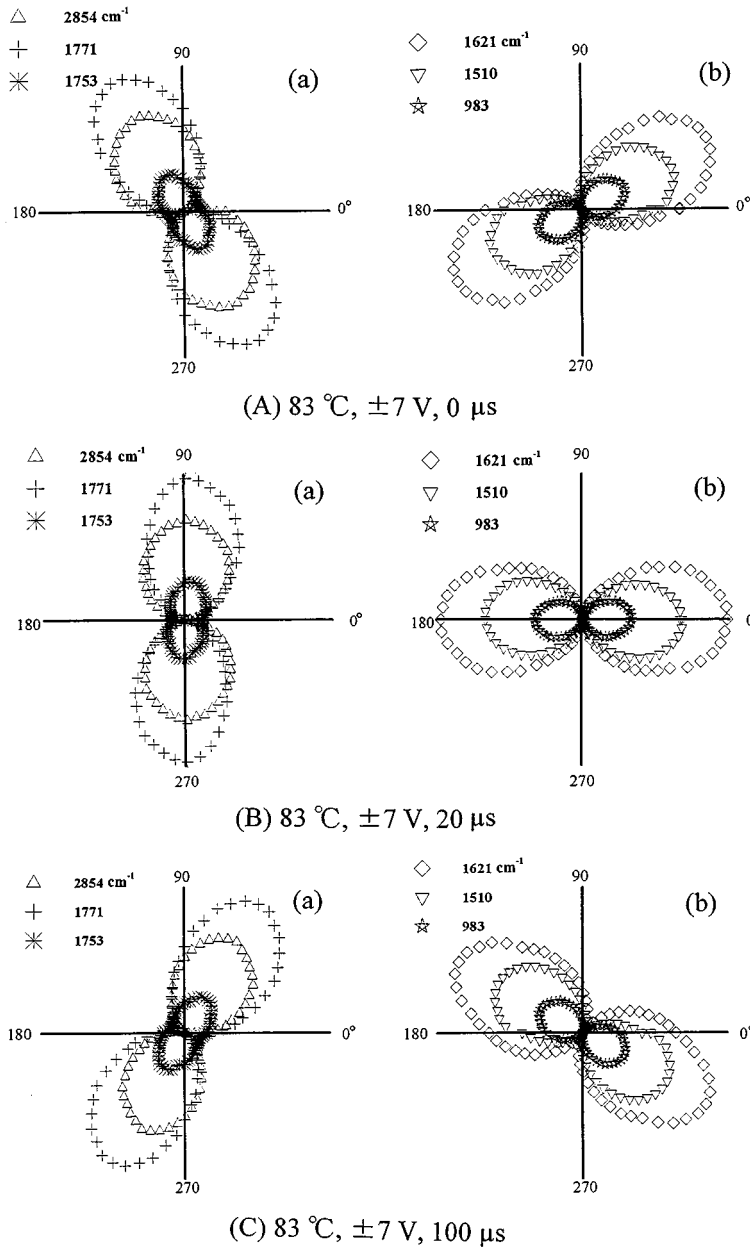
(A) 83 °C, ±7 V, 0 μs

(B) 83 °C, ±7 V, 20 μs

FIG. 8. Polar plots of peak absorbance $A(\omega)$ vs the polarization angle ω before and during the dynamical switching of the VOH8 in the Sm-C^* phase at 0, 20, and 100 μs at 83 °C and applied voltage pulse of ±7 V and 5 kHz repetition rate for the selected bands characterizing (a) the alkyl chain and the C=O groups, (b) the mesogen segment.

(C) 83 °C, ±7 V, 100 μs

neous polarization, respectively [6]. Both $\gamma_\varphi(T)$ and $P(T)$ decrease with increasing temperature but γ_φ varies more rapidly than P and thus would affect τ at different temperatures. However, it is the ferroelectric torque density ($\sim \mathbf{P} \cdot \mathbf{E}$) which, for moderate fields is larger than the dielectric torque density ($\sim \Delta \epsilon_0 E^2$), and thus determines the response time in which the FLC's give rise to the field-induced reorientation of $\mathbf{n}$ on the tilt cone. Thus one can understand, at least qualitatively, the observed shorter reorientation times for all the segments at higher temperatures and electric field strengths. The hydrogen-bonded C=O group moves with the mesogen and reorients at a faster rate at the employed temperatures and voltages compared to the alkyl chain and the free C=O group. However, these theoretical relations are applicable for the molecules which are presumed to reorient as a rigid unit, and it is therefore not feasible to estimate the reorientation rates of individual segments.

We quantify the field-induced orientation rates by plotting the normalized peak intensity vs polarization angle at three delay times of 0, 20, and 100 μs at 83 °C and 75 °C and ±7 V. A plot at 83 °C is shown in Fig. 8. A closer look at these polar plots indicates that the magnitudes of the absorbance changes in the 0–20 μs range are slightly larger for the C=O bands than in the 20–100 μs range, while for other bands, the changes are of nearly similar magnitude. Moreover, the transition dipoles of the C=O groups have moved with a net change in their orientation of 64°, which is larger than those of the core bands (60°), while the transition dipole of the CH$_2$ stretching mode has moved by a smaller amount (55°) after the orientation is finished. This trend is consistent with the static data and clearly indicates that the alkyl chains move at a slower rate compared to the mesogen and chiral groups, even during the dynamical switching.

IV. CONCLUSIONS

The various investigations carried out previously on chiral ferroelectric liquid crystals have indicated that the mesogen

and the alkyl chains reorient simultaneously as rigid units at the same rate during electro-optical switching. However, our polarization-dependent IR studies under applied dc electric fields and the time-resolved polarized IR measurements during the course of switching between the surface-stabilized states of the chiral ferroelectric liquid crystal VOH8 in the smectic-C^* phase have revealed the following significant information.

The average alkyl chain and the mesogen axis do not coincide with each other in the equilibrium state, and the alkyl chains are less tilted than the cores with respect to the smectic layer normal.

The motion of the carbonyl group is strongly hindered, and the distribution function for the C=O group is not cylindrically symmetric around the long mesogen axis.

During switching between the two surface-stabilized states, the hydrogen-bonded C=O group and the core move together and reach their equilibrium orientation at a faster rate than the alkyl chain at all the temperatures and voltages employed in this study.

ACKNOWLEDGMENTS

[1] S. T. Lagerwall, N. A. Clark, J. Dijon, and J. F. Clerc, Ferroelectrics **94**, 3 (1989).

[2] N. A. Clark, and S. T. Lagerwall, Appl. Phys. Lett. **36**, 899 (1980).

[3] N. A. Clark, and S. T. Lagerwall, Ferroelectrics **59**, 25 (1984).

[4] S. Matsumoto, A. Maruyama, H. Hatho, Y. Kinoshita, H. Harai, M. Ishikawa, and S. Kamagani, Ferroelectrics **85**, 235 (1988).

[5] J. Dijon, in *Liquid Crystals, Application and Uses*, edited by B. Bahadur (World Scientific, Singapore, 1990), Vol. 1, p. 305.

[6] J. W. Goodby, R. Blinc, N. A. Clark, S. T. Lagerwall, M. A. Osipov, S. A. Pikin, T. Sakurai, K. Yoshino, and B. Zeks, *Ferroelectric Liquid Crystals: Principles, Properties and Applications* (Gordon and Breach, Philadelphia, 1991).

[7] H. Toriumi, H. Sugisawa, and H. Watanabe, Jpn. J. Appl. Phys., Part 2 **27**, L935 (1988).

[8] V. G. Gregoriu, J. L. Chao, H. Toriumi, and R. A. Palmer, Chem. Phys. Lett. **179**, 491 (1991).

[9] H. Sugisawa, H. Toriumi, and H. Watanabe, Mol. Cryst. Liq. Cryst. **214**, 11 (1992).

[10] T. Urano and H. Hamaguchi, Chem. Phys. Lett. **195**, 287 (1992).

[11] T. Takano, T. Yokoyama, and H. Toriumi, Appl. Spectrosc. **47**, 1354 (1993).

[12] H. Sasaki, M. Ishibashi, A. Tanaka, N. Shibuya, and R. Hasegawa, Appl. Spectrosc. **47**, 1390 (1993).

[13] T. Urano and H. Hamaguchi, Appl. Spectrosc. **47**, 2108 (1993).

[14] S. V. Shilov, S. Okretic, and H. W. Siesler, Vib. Spectrosc. **9**, 57 (1995).

[15] K. Masutani, H. Sugisawa, A. Yokota, Y. Furukawa, and M. Tasumi, Appl. Spectrosc. **46**, 560 (1992).

[16] K. Masutani, A. Yokota, Y. Furukawa, M. Tasumi, and A. Yoshizawa, Appl. Spectrosc. **47**, 1370 (1993).

[17] M. Czarnecki, N. Katayama, Y. Ozaki, M. Satoh, K. Yoshio, T. Watanabe, and T. Yanagi, Appl. Spectrosc. **47**, 1382 (1993); N. Katayama, M. A. Czarnecki, M. Satoh, T. Watanabe, and Y. Ozaki, *ibid.* **51**, 487 (1997).

[18] M. Czarnecki, N. Katayama, M. Satoh, T. Watanabe, and Y. Ozaki, J. Phys. Chem. **99**, 14 101 (1995).

[19] N. Katayama, M. A. Czarnecki, Y. Ozaki, K. Murashiro, M. Kikuchi, S. Saito, and D. Demus, Ferroelectrics **147**, 441 (1993).

[20] N. Katayama, T. Sato, Y. Ozaki, K. Murashiro, M. Kikuchi, S. Saito, D. Demus, T. Yuzawa, and H. Hamaguchi, Appl. Spectrosc. **49**, 977 (1995).

[21] S. V. Shilov, S. Okretic, H. W. Siesler, R. Zentel, and T. Oge, Macromol. Rapid Commun. **16**, 125 (1995).

[22] M. A. Czarnecki, S. Okretic, and H. W. Siesler, J. Phys. Chem. B **101**, 374 (1997).

[23] S. V. Shilov, S. Okretic, H. W. Siesler, and M. A. Czarnecki, Appl. Spectrosc. Rev. **31**, 82 (1996).

[24] F. Hide, N. A. Clark, K. Nito, A. Yasuda, and D. M. Walba, Phys. Rev. Lett. **75**, 2344 (1995).

[25] K. H. Kim, K. Ishikawa, H. Takezoe, and A. Fukuda, Phys. Rev. E **51**, 2166 (1995).

[26] B. Jin, Z. Ling, Y. Takanishi, K. Ishikawa, H. Takezoe, A. Fukuda, M. Kakimoto, and T. Kitazume, Phys. Rev. E **53**, R4295 (1996).

[27] K. H. Kim, K. Miyachi, K. Ishikawa, H. Takezoe, and A. Fukuda, Jpn. J. Appl. Phys., Part 1 **33**, 5850 (1994).

[28] Y. Tian, X. Xu, Y. Zhao, X. Tang, F. Su, X. Zhao, and E. Zhou, Liq. Cryst. **19**, 295 (1995).

[29] N. B. Colthup, L. H. Daly, and S. E. Wiberley, *Introduction to Infrared and Raman Spectroscopy* (Academic, New York, 1975), Chaps. 8 and 9.

[30] J. K. Moscicki, and S. Urban, Mol. Cryst. Liq. Cryst. **59**, 73 (1980).

[31] H. Sapper, D. C. Cameron and H. H. Mantsch, Can. J. Chem. **59**, 2543 (1981).

[32] J. Michl and E. W. Thulstrup, *Spectroscopy with Polarized Light, Solute Alignment by Photoselection in Polymers, Liquid Crystals, and Membranes* (VCH Verlasgsgesellschaft, Weinheim, 1986).